Malaysian Journal of Chemistry, 2023, Vol. 25(3), 260-274
(Special Issue: *Rubbercon2022*)

Effect of Zein Protein on Rheological and Hydrophobicity of Gellan Gum-based Food Packaging Film

Yin Yin Thoo*, Ru Wei Teoh and Adeline Su Yien Ting
School of Science, Monash University Malaysia, Jalan Lagoon Selatan, 47500 Bandar Sunway Selangor, Malaysia
*Corresponding author (e-mail: thoo.yin.yin@monash.edu.my)

Alternative food packaging materials derived from polysaccharides can potentially reduce the use of plastic material. Gellan gum (GG) is a polysaccharide with good film-forming properties (FFS) but is limited by its hydrophilic nature and poor barrier properties. Therefore, GG film was blended with hydrophobic zein protein to improve overall film hydrophobicity and barrier properties. This study aims to investigate the effect of incorporating hydrophobic zein protein on film hydrophobicity as well as film rheological, molecular and barrier properties. Zein/GG FFS exhibited shear thinning behaviour and increasing zein concentration increases viscosity. Zein/GG FFS also shows 'true-gel' behaviour, whereby G′ has a minimal dependency on angular frequency. Surface hydrophobicity is significantly ($p<0.05$) improved, as the water contact angle increased by 18.3° after zein addition. Moreover, the water vapour permeability reduced from 10.71×10^{-4} gmmm^{-2}h^{-1}kPa^{-1} to 7.96×10^{-4} gmmm^{-2}h^{-1}kPa^{-1} and oxygen permeability reduced from 30.89 mmolkg^{-1} to 22.38 mmolkg^{-1} following the addition of zein. These observations are likely due to the hydrophobic nature of zein, which repels water and favors the formation of intermolecular bonds (hydrogen bonds and electrostatic interactions). Overall, the incorporation of zein imparts favourable changes to film microstructure and this improves hydrophobicity and barrier properties of GG film.

Keywords: Barrier properties; biodegradable film; film hydrophobicity; gellan gum; zein

Received: January 2023; Accepted: March 2023

Single-use plastic food packaging materials have become a global issue as plastic packaging derived from petroleum-based materials are not biodegradable and harmful to the environment. Therefore, it is of great importance to develop food packaging that is renewable and biodegradable. Natural biopolymers, such as polysaccharides, proteins and lipids have gained considerable attention in producing biodegradable food packaging film, owing to their abundance in nature, low health risk, good biodegradability and biocompatibility [1]. Among the many natural biopolymers, gellan gum (GG) received much interest recently, as GG has good gelling and film-forming properties, which makes it a promising material for use in the medical, pharmaceutical, and food industries [2, 3].

GG is a water-soluble and anionic polysaccharide produced by *Sphingomonas elodea*. It is made up of repeating units of tetrasaccharides, which are two residues of D-glucose and one residue for each D-glucuronic acid and L-rhamnose [4]. In the native form, GG has a large number of acyl groups and is known as high-acyl GG (HAGG). GG is commonly used as thickening, gelling agent and stabilizer to improve food product quality [5]. Besides, GG can also improve the quality of tissue scaffold [6], increase effectiveness in therapeutic effect on rheumatoid arthritis [7] and act as an anti-adhesion barrier [8]. Although GG is shown to be a promising material as hydrogel in pharmaceutical and medical industry, its application in food packaging film is limited due to poor water-resistance and barrier properties. Thus, GG is blended with other naturally occurring biopolymer or inorganic nanoparticles to improve the water-resistance and barrier properties. The addition of montmorillonite clay to GG/agar composite film improves the overall water-resistance [9]. Besides, incorporation of alginate into GG film result in a synergistic effect which enhanced the water resistance of alginate/GG composite film on paper cups for hot drinks [10]. Blending GG with *k*-carrageenan and xanthan gum, significantly improved the water vapour permeability and the resulting blended film had a low moisture content [11].

Aside from blending with other polysaccharides to improve water-resistance, the incorporation of zein protein could further enhanced water-resistance. Zein is a hydrophobic plant storage protein, isolated from endosperm of corn kernels. The hydrophobicity of zein is attributed to the presence of high proportion of hydrophobic amino acids, such as glutamine and proline, which caused zein to be water-insoluble but alcohol-soluble [12, 13]. Although zein resulted in a film with poor mechanical properties, the presence of

†Paper presented at Rubbercon2022

these hydrophobic amino acids contributed to the excellent water-resistance performance and low gas permeability [14, 15, 16]. Moreover, zein is a by-product from corn processing method which can be obtained abundantly at low prices. Therefore, zein has become a popular compound and has great potential in production of composite or blended film with other biopolymers. Similarly, the addition of zein to chitosan improved the water vapour permeability as well as reduced moisture content and water absorbency of composite film [17]. In addition, blending of zein with pre-gelatinized maize starch improves water vapour permeability and mechanical properties of starch film [18]. These findings suggest that the incorporation of zein is likely to improve water vapour permeability and barrier properties of polysaccharide film. Thus, blending zein with GG film may improve water-resistance and reduce gas permeability as compared to pure GG film. To the best of our knowledge, zein-loaded GG film has not been investigated and this study is the first few to establish this.

Therefore, the aim of this study is to investigate the effect of zein protein on water-resistance and gas barrier properties of GG film. Different proportions of zein were added into GG film and its effect on rheological properties (steady shear analysis and dynamic rheology), mechanical properties (puncture force and deformation), water-resistance performance (water contact angle, swelling ratio and total soluble matter) and barrier properties (water vapour permeability and oxygen permeability) were determined. Nano-analytical tools were used to elucidate the underlying interaction between zein and GG, in which, these includes atomic force microscopy (AFM) (3D surface topography and surface roughness), field emission scanning electron microscopy (FESEM) (surface morphology), X-Ray diffraction (XRD) (XRD pattern and crystallinity index) and attenuated total reflection – fourier transform infrared (ATR-FTIR) spectroscopy (intermolecular bonding).

MATERIALS AND METHODS

Chemicals and Materials

High-acyl GG (M_w = 1-2 × 10^6 Daltons, Kelcogel LT100, CP Kelco) was obtained as a gift from Brenntag Sdn. Bhd. (Shah Alam, Malaysia). Zein (M_w = 20 kDa), anhydrous Calcium Chloride ($CaCl_2$), Magnesium nitrate hexahydrate ($Mg(NO_3)_2 \bullet 6H_2O$), glycerol, absolute ethanol, chloroform, acetic acid, potassium iodide and sodium thiosulphate were purchased from Sigma-Aldrich (St. Louis, MO. USA).

Preparation of zein-loaded GG Film

Zein-loaded GG films were fabricated using solvent casting method. GG powder (0.5 g) was dissolved in 100 ml distilled water at 80 °C, under continuous stirring for 20 min to ensure complete dissolution. Then, anhydrous $CaCl_2$ (0.02 g; 4% based on amount of GG powder, w/w) was added into GG solution and continued stirring for 1 h. Followed by the addition of 300 µL (0.3% based on total GG solution, v/v) glycerol and stirred for 20 min.

Prior to adding zein solution into GG solution, zein powder (0.5 g) was dissolved in 80% ethanol solution (100 mL) at room temperature for 2 h under continuous stirring. Zein solution was then added dropwise into GG solution by using a burette at 80 °C, under 700 rpm for 30 min, to ensure consistency [53]. Four different concentrations of zein were prepared, ranging from 5% to 20% (dry weight of zein:dry weight of GG, w/w). The zein/GG film forming solution (FFS) (50 mL) was then carefully poured onto petri dishes and dried in an oven at 45 °C for 24 h. Composite films were formed when the water in zein/GG FFS was completely evaporated.

Rheological Properties of GG/zein FFS

Steady state analysis and dynamic viscoelastic properties of zein/GG FFS were performed on a stress-controlled rheometer (MCR 302 SN82434519, Anton Paar GmbH, Graz, Austria). Concentric cylinder geometry (CC27 SN51692, 26.6 mm bob diameter, 28.9 mm cup diameter and no gap) was fitted onto the rheometer to carry out steady state analysis, while parallel plate geometry (PP50/S SN53309, 49.9 mm plate diameter and 1 mm gap) was fitted to determine dynamic viscoelastic properties. Triplicates were done for all samples and all analyses were performed at 24°C.

Steady State Analysis

The flow curves and viscosity of different zein concentrations in FFS were obtained within a range of shear rates from 0.1 to 100 1/s. The experimental data were then fitted onto the Power-law model (Eq. (1)) [19].

$$\tau = \kappa_p(\dot{\gamma})^{n_p} \quad (1)$$

Where τ is shear stress (Pa); $\dot{\gamma}$ is shear rate (1/s); κ_p is power-law consistency coefficeint (Pa.s^n) and n_p is power-law flow behaviour index (dimensionless).

Dynamic Viscoelastic Properties

In order to elucidate the dynamic viscoelastic properties of zein/GG FFS, frequency sweep test was performed. Prior to this test, the linear viscoelastic (LVE) range was determined and 5% shear strain (within the LVE range) was applied for all measurements. All zein/GG FFS with different zein concentrations were analyzed within the angular frequency range of 0.1 to 100 rad/s. The mechanical spectra were obtained, which include dynamic rheological parameters of storage modulus (G′), loss modulus (G″) and complex viscosity (|η*|)

[20]. The correlation of Power-law between G′ and angular frequency (rad/s) were determined using Eq. (2):

$$G' = k' \times \omega^n \quad (2)$$

Where G′ is storage modulus; k′ is model constant (consistency index); n is slope of frequency dependency of G′ (flow behaviour index) and ω is angular frequency (rad/s).

Water Contact Angle (WCA)

WCA of composite film were performed through sessile drop method, using ramé-hart Model 250 goniometer (ramé-hart, Succasunna, New Jersy, USA). A drop of distilled water (4 μL) was placed on top of composite films and repeated at five random places. The WCA and images were recorded after one min, using DROPimage Advanced (ramé-hart, Succasunna, New Jersy, USA) software [21].

Swelling Ratio and Total Soluble Matter (TSM)

Zein-loaded GG films were cut into 2 cm × 2 cm square pieces and weighed before immersing them into distilled water for 24 h. The composite films were weighed again after 24 h to determine swelling ratio. The swelled composite films were then dried at 50 °C until a constant weight was reached. The final constant weight was recorded to determine TSM. Five replicates were performed for each zein concentration. The swelling ratio and TSM of composite films were calculated through the following equation (Eq. (3), (4)):

$$Swelling\ ratio\ (\%) = \frac{W_f - W_i}{W_i} \times 100 \quad (3)$$

Where W_f and W_i were final and initial weights of the composite film, respectively.

$$TSM\ (\%) = \frac{W_i - W_d}{W_i} \times 100 \quad (4)$$

Where W_i and W_d were initial and after drying weights of the composite film, respectively.

Water Vapour Permeability (WVP) and Oxygen Permeability (OP)

The WVP of composite films were determined according to ASTM E-96 gravimetric method. Magnesium nitrate was added into desiccator 24 h before WVP tests were performed, to achieve 54% relative humidity (RH). Anhydrous calcium chloride (40 g) was added into crystallising dish (2 cm air-gap) and covered with composite films. The edge and sides of crystallizing dishes were sealed completely by applying Vaseline and covered with parafilm to limit the entrance of water vapour. Then, the prepared test sets were placed in a desiccator for 5 h and the weight was recorded for every 30 min. Triplicates were carried out for each zein concentration.

The experimental data recorded was water vapour transmission rate (WVTR) in g m^{-2} h^{-1} unit (Eq. (5)) and the WVP (g mm kPa^{-1} m^{-2} h^{-1}) results were calculated using Eq. (6).

$$WVTR = \frac{\Delta m}{tA} \quad (5)$$

$$WVP = \frac{\Delta m}{tA} \times \frac{L}{S(RH_{over} - RH_{under})} \quad (6)$$

Where $\frac{\Delta m}{t}$ represents the slope of linear regression between weight of crystallising dish and time (g/h). A represents the exposed film surface area (m^2). L represents composite film thickness (mm). S represents the saturated water vapour pressure (kPa). RH_{over} and RH_{under} represents RH (%) above composite film and under composite film, respectively.

OP indicates the ability of composite films in controlling oxygen transfer. Sunflower oil (15 mL) was added into crystallising dish and covered with composite films. Similar with WVP, the edge of cystallising dishes were sealed completely by using Vaseline and parafilm. A negative control with only sunflower oil was used in this study. All prepared test sets were incubated at 50 °C for seven days. Peroxide values (PV; m mol kg^{-1}) of sunflower oil were determined according to AOCS official method (Cd 8-53) after the incubation period [22].

Mechanical Properties

Puncture tests were performed using TA XT Plus texture analyzer (Stable Microsystems, Surrey, England). Zein-loaded GG films were cut into 2 cm × 2 cm squared samples and fixed on the stage. After that, composite film samples were perforated by a cylindrical probe (2 mm diameter and moving speed of 8.3 mm/s) [23]. Puncture force and deformation were determined from the curves of force and deformation, analyzed using Exponent software (Stable Microsystems, Surrey, England) with five replicates for each zein concentration.

Microstructure of Film

Field-emmision Scanning Electron Microscopy (FESEM) Analysis

FESEM (Hitachi SU8010, Hitachi, Minato-ku, Tokyo, Japan) was used to study the morphology of zein-loaded GG film. Composite films were cut into 3 mm × 3 mm small squares and platinum-sputter-coated. All composite films with different zein concentrations were examined with an accelerating voltage of 2.0 kV and × 5.00k magnification.

Atomic Force Microscopy (AFM) Analysis

AFM (Multimode 8, Bruker, Billerica, Massachusetts, USA) with tapping mode and silicon nitride probes of resonance frequency at 70 kHz and a spring constant of 0.4 N/m was used in this study. Composite films of 3 mm × 3 mm small squares were prepared and two areas of 5μm × 5μm from the small squares were scanned at a speed of 0.8Hz with a resolution of 512 × 512 pixels. The 3D surface topographic images of composite films were captured. Besides, the roughness of film surface was calculated using arithmetic average of surface roughness (R_a, Eq. (7)) and root mean square of surface roughness (R_q, Eq. (8)), using Nanoscope Analysis 1.7 (Bruker, Billerica, Massachusetts, USA) software and flattened with 3rd order.

$$R_a = \frac{1}{N}\sum_{i=1}^{N}|Zi| \quad (7)$$

$$R_q = \sqrt{\frac{\sum(\mathrm{Zi})^2}{N}} \quad (8)$$

Where N is the number of points in the image, while Zi is the height deviaiton from mean of heights [24].

X-ray Diffraction (XRD) Analysis

The XRD patterns were recorded using D8 Discovery diffractometer (Bruker, Billerica, Massachusetts, USA) with CuKα radiation at 40 kV and 40 mA and at a scan rate of 2°/min, in the range of 2θ from 5° to 55° [25]. Prior to analysis, composite films were cut into ten 1.5 cm × 1.5 cm squares and stacked on top of each other to form 10 - layered thick sample. The crystallinity values of composite films were determined through DIFFRAC.EVA software (version 4.2.1, Bruker, Billerica, Massachusetts, USA).

Attenuated Total Reflection – Fourier Transform Infrared (ATR-FTIR) Spectroscopy *Analysis*

The spectra of zein-loaded GG film were recorded on Spectrum Two FT-IR spectrometer (PerkinElmer, Waltham, Massachusetts, USA). All composite films were run using ATR accessory, in the range of 4000 – 400 cm^{-1} with 32 scans and a resolution of 4 cm^{-1}.

Statistical Analysis

The water-resistance performance, barrier and mechanical properties of all composite films were statistically analysed and compared using SPSS (SPSS Inc, Chicago, IL, USA) by one-way analysis of variance (ANOVA). Tukey's test were performed to compare all the means and significant differences were determined at $P < 0.05$.

RESULTS AND DISCUSSION

Steady Shear Analysis

Steady shear analysis was performed to investigate the effect of different zein concentrations on viscosity of zein/GG FFS. From Figure 1, all zein concentrations (0 – 20%) exhibit a similar trend, where the viscosity decreases when shear rate increases. This is typical for a pseudoplastic fluid as a fluid showed shear-thinning behaviour when shear rate increased. Thus, zein/GG FFS remained as a pseudoplastic fluid for all zein concentrations and exhibited shear thinning behaviour. For low shear rates, the viscosity is similar for all zein concentrations. While at a higher shear rate, zein/GG FFS added with 20% zein remained at the lowest viscosity, as compared to other zein concentrations. This implies that the addition of zein influence shear thinning behaviour. Similar findings were also observed when zein is incorporated into the agar/ konjac glucomannan system and the blends exhibited shear-thinning behaviour while the viscosities decreases when shear rate increases [26].

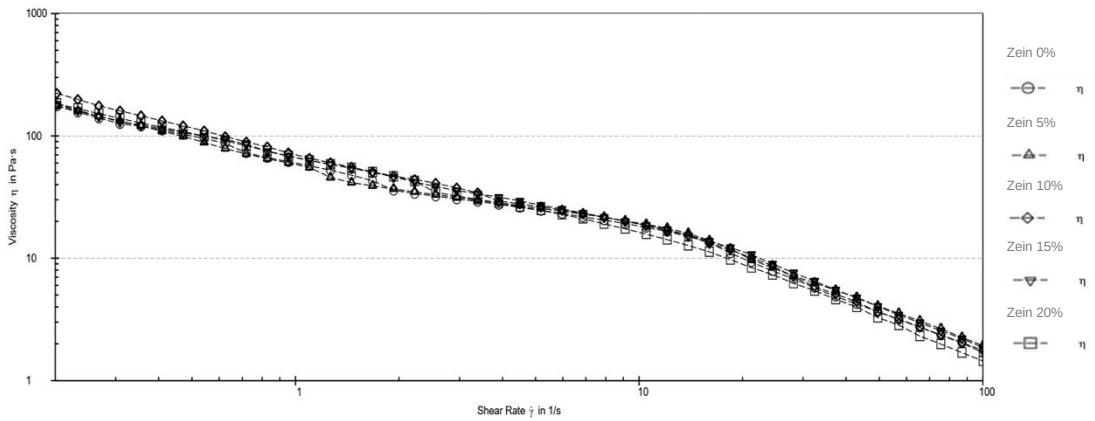

Figure 1. Viscosity (Pa • s) of zein/GG FFS incorporated with various zein concentration (5-20%) within a shear rate of 0.1 – 100 1/s.

The shear-thinning behaviour of zein/GG FFS was further confirmed by fitting the experimental data to power law model. The parameters from power law model are consistency index, K, and flow behaviour index, n. Consistency index describes the specific viscosity at a specific point of shear rate, while flow behaviour index explains the tendency of a system to flow. If the flow behaviour index is less than 1, the system exhibit elastic behaviour; if is more than 1, the system exhibits viscous behaviour [27]. As seen in Table 1, the consistency index of zein/GG FFS increases when the concentration of zein increases. The incorporation of high zein concentrations, 10% and 20% zein, results in a higher viscosity of zein/GG FFS. A similar trend is also observed in the flow behaviour index. Where addition of 10% and 20% zein significantly ($p<0.05$) increase the flow behaviour index from 0.679 to 0.742. Since all the zein concentration from zein/GG FFS has a flow behaviour index of less than 1, this FFS predominantly has elastic behaviour. Similar effect of zein was observed when added into *Tremella fuciformis* polysaccharide (TPS) solution. The viscosity is higher when proportion of zein increases, indicated by increasing consistency index and all mixtures have flow behaviour index of less than 1, which shows a pseudoplastic fluid [28]. Nevertheless, all the results have good fitting with the power law model with high correlation (0.9759 – 0.9836).

Table 1. Power law model with parameters of consistency index, K, and flow behaviour index, n, performed on steady shear test with various zein concentrations (5 – 20%).

Sample	Consistency index, K	Flow behaviour index, n	R^2
GG	61.60 ± 2.10^{c}	0.68 ± 0.02^{b}	0.98
GGZ 5%	63.90 ± 0.50^{c}	0.67 ± 0.01^{b}	0.98
GGZ 10%	77.30 ± 5.90^{a}	0.73 ± 0.01^{a}	0.98
GGZ 15%	67.00 ± 2.60^{cb}	0.68 ± 0.01^{b}	0.98
GGZ 20%	74.60 ± 4.80^{ab}	0.74 ± 0.01^{a}	0.98

$^{a-c}$ represents statistically significant differences of consistency index, k, and flow behaviour index, n, of GG solution incorporated with various zein concentrations (5 – 20%). The values stated were mean ± standard deviation. Triplicates were performed for each samples.

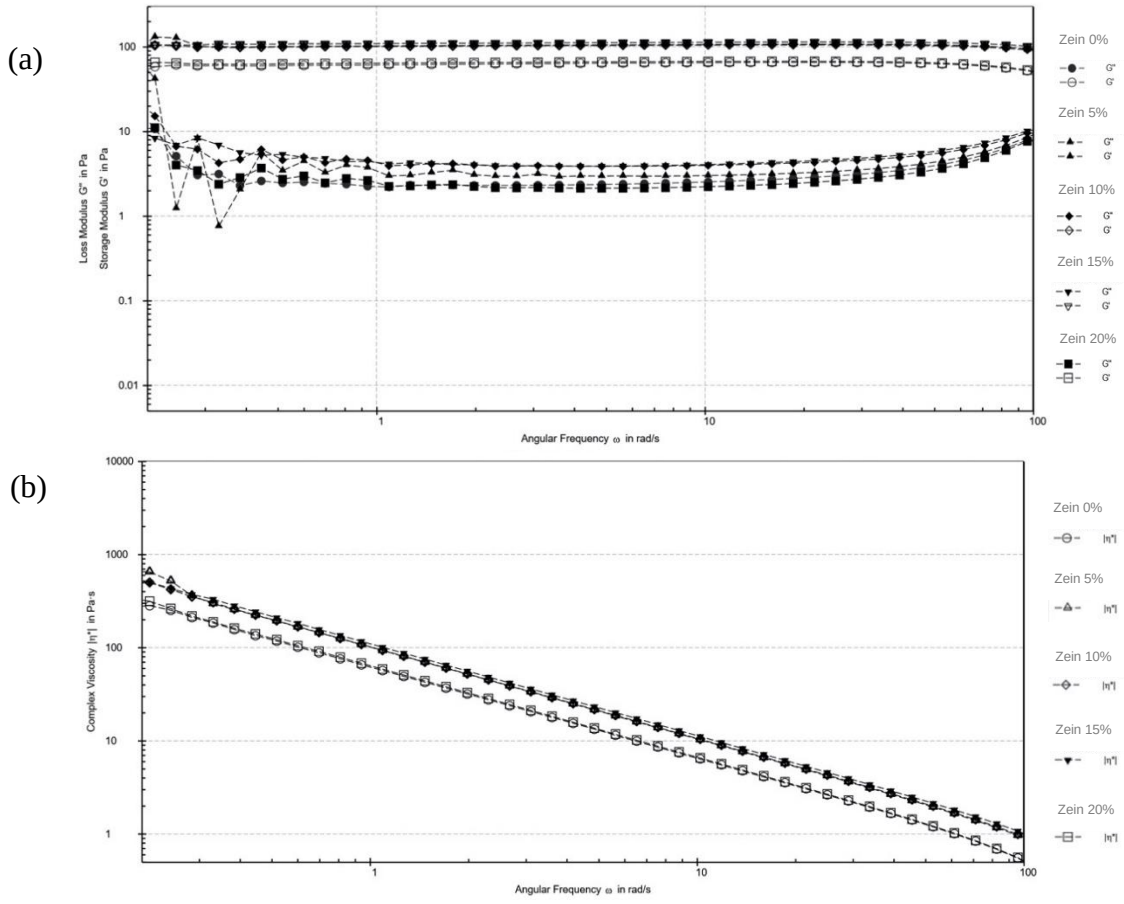

Figure 2. (a) Frequency sweep test (0.1 – 100 rad/s) and **(b)** Complex viscosity of GG solution incorporated with various zein concentrations (5-20%). Blanked symbols represent storage modulus (G′); Filled symbols represent loss modulus (G″).

Dynamic Rheological Properties

A frequency sweep test is performed within the LVE region, with a constant strain of 5% to determine the dependency of G′, G″ and complex viscosity, |η*|, on frequency. The effect of zein concentrations on the mechanical structure and behaviour of zein/GG FFS is investigated through this test. From Figure 2(a), all zein concentrations (0-20%) from zein/GG FFS has higher G′, compared to G″. This phenomenon indicates that zein promoted entanglement with GG polymer and behaves as a typical gel [29]. Increasing zein concentration from 5 to 15% enhanced the structural network between GG and zein with higher G′. Since incorporation of zein into GG solution exhibited a typical gel behaviour, all zein concentration in zein/ GG FFS behaves as 'true-gel'. A study involving adding zein into konjac glucomannan FFS promotes formation of gel from solution and this change is attributed to the entanglement between zein and konjac glucomannan molecules [30]. Aside from behaving as a 'true gel', G′ of zein/GG FFS shows low frequency dependency across 0.1 to 100 rad/s and G′ only starts to decrease at a higher frequency range near 100 rad/s. This indicates a typical characteristic of a strong gel.

The complex viscosity of zein/GG FFS for all zein concentrations decreases as the frequency increase. These results are similar to the steady shear behaviour, whereby all zein/GG FFS are pseudoplastic fluid since they exhibit shear-thinning behaviour. This is due to GG and zein polymer are oriented along the streamlined flow and disengagement of entangled zein/GG network could not restore in time at a higher shear rate. In addition, the concentration of zein will affect the complex viscosity of zein/GG mixture. As seen in Figure 2(b), the complex viscosity of mixture with 5 to 15% of zein is higher than GG solution. This is attributed to the development of intermolecular bonding between GG and zein and a stronger intermolecular polymer network is formed. Thus, higher complex viscosity is obtained when zein concentration increases. Study shows that increasing zein concentration in zein-based film results in higher viscosity and this could possibly be due to the different degree of unfolding and aggregation in zein [31].

In order to understand zein/GG network structure and behaviour thoroughly, experimental data from complex viscosity are fitted into power-law model. Similar to steady shear behaviour, zein/GG FFS with different zein concentrations showed a good correlation (R^2) of 0.9947 to 0.9988 between experimental and calculated values. The flow behaviour index, n, is similar across all zein concentrations and since all the values are less than 1, zein/GG FFS has elastic behaviour. Furthermore, addition of zein increases the consistency index of GG solution significantly ($p<0.05$) from 64.5 to 107.6, which indicates an increase in viscosity when concentration of zein increases. However, a further increment to 20% zein concentration results in a decrease in viscosity and a lower consistency index.

Surface Hydrophobicity

The WCA is a good indicator in determining the surface hydrophobicity of zein-loaded GG film. The goniometer images (Figure 3) depicts the CA of a water droplet on GG film incorporated with various zein concentration at 1 min. The WCA increased significantly ($p < 0.05$) at 10% zein, which is 97.5°, as compared to 0% and 5% zein, which is 83.6° and 84.0° respectively. Further addition of zein to 20% had the highest ($p < 0.05$) WCA of 101.9°.

Table 2. Power law model with parameters of consistency index, K, and flow behaviour index, n, performed on frequency sweep test with various zein concentrations (5 – 20%).

Sample	Consistency index, K	Flow behaviour index, n	R^2
GG	64.50 ± 2.30^{b}	0.99 ± 0.01^{a}	0.99
GGZ 5%	97.00 ± 11.80^{a}	1.00 ± 0.01^{a}	0.99
GGZ 10%	98.10 ± 5.50^{a}	1.00 ± 0.01^{a}	0.99
GGZ 15%	107.60 ± 2.90^{a}	1.00 ± 0.01^{a}	0.99
GGZ 20%	61.40 ± 3.30^{b}	1.00 ± 0.01^{a}	0.99

$^{a-b}$ represents statistically significant differences of consistency index, k, and flow behaviour index, n, of GG solution incorporated with various zein concentrations (5 – 20%). The values stated were mean ± standard deviation. Triplicates were performed for each samples.

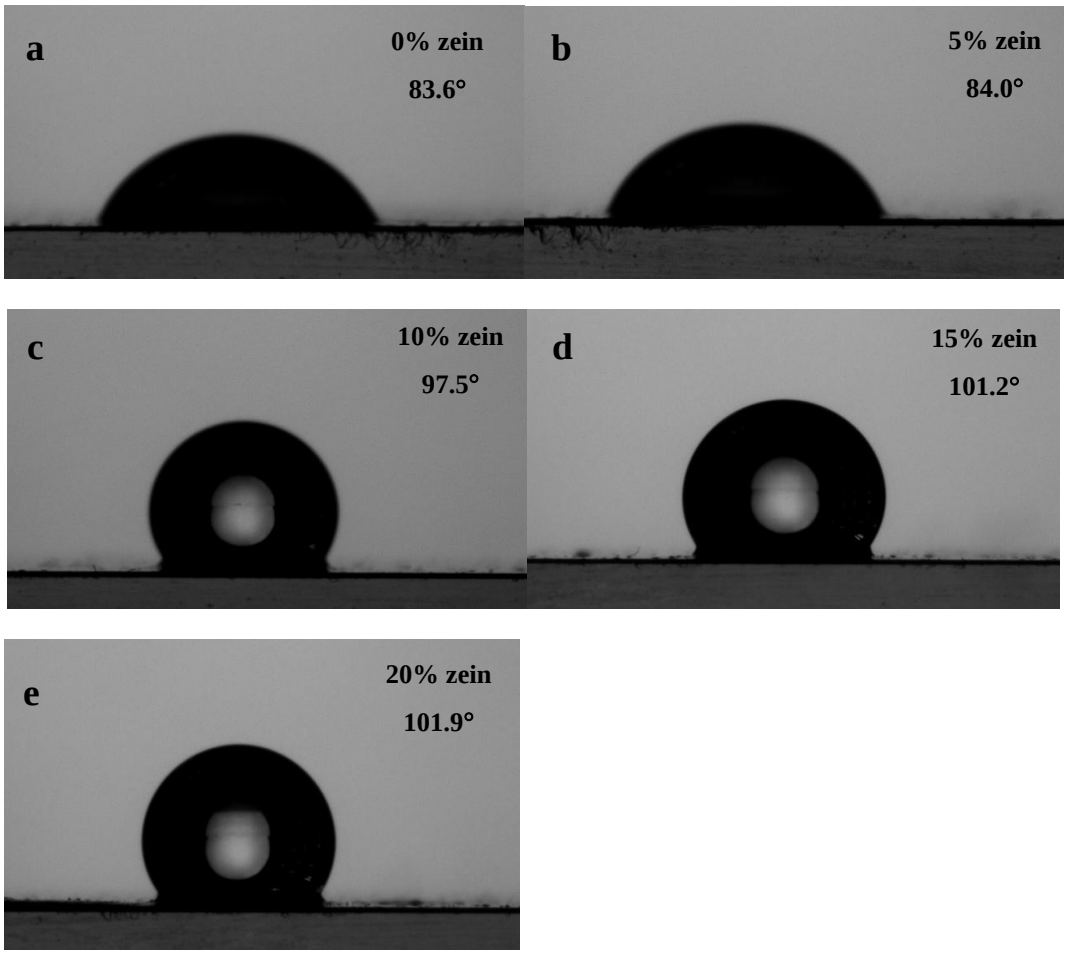

Figure 3. Goniometer images of WCA of water droplet at 1 min. **(a)** 0% zein (pure GG film); **(b)** 5% zein + GG film; **(c)** 10% Zein + GG film; **(d)** 15% zein + GG film; **(e)** 20% zein + GG film.

Generally, a surface is considered hydrophobic when the static water CA is above 90.0° and is considered hydrophilic when the static water CA is below 90.0° [32]. The control film fabricated with the GG has a CA of 83.6°, indicating its hydrophilic surface that attribute to the hydrophilic nature of GG. The addition of zein at the concentration of 10% improved the hydrophobicity of the film surface, where CA increased to above 90.0°. This suggests that zein-loaded GG film has a more compact structure and obstructs the diffusion of water molecules into the zein-loaded GG film when water was dropped onto the surface. Thus, increase the hydrophobicity of composite film [33]. Similarly, addition of corn zein improves the surface hydrophobicity, whereby the water CA of cellulose nanocrystals/corn zein composite film increases as the proportion of corn zein was increased [34]. Increasing zein concentration on potato starch-olive oil edible films further improves the surface hydrophobicity, in which the WCA was reported to be close to 100° [35].

Table 3. WCA (°) of GG film incorporated with various zein concentrations (0% - 20%) at 1 min.

Concentration of zein (%)	Water contact angle ± SD (°)
0 (Control)	83.6 ± 0.9^{c}
5	84.0 ± 1.5^{c}
10	97.5 ± 4.1^{b}
15	101.2 ± 1.1^{ba}
20	101.9 ± 2.1^{a}

^{abc} represents statistically significant differences in water contact angle for zein-loaded GG film at various concentrations (0% - 20%) at $p < 0.05$; Values stated were mean ± SD with five replicates.

Swelling Ratio and TSM

The swelling ratio of film implies how well a film absorbs and retains water. Our findings show that the incorporation of zein increased the swelling ratio. As seen in Table 4, pure GG film has the lowest swelling ratio of 12,791% as compared to all zein concentrations. The swelling ratio increases with the increasing concentration of zein from 5% to 15%. Notably, addition of 20% of zein decreased the swelling ratio. This is likely attributed to the hydrophobic zein, where water molecules displace zein particles from the intermolecular interaction between GG. This is in good accordance with the FTIR in this study, where zein interacts with GG through hydrogen bonding and electrostatic interaction. In addition, zein repels water and tends to aggregate if present in an aqueous environment. Therefore, this may result in GG film having more free OH groups, which is more likely to form hydrogen bonds with water molecules.

TSM describes the total amount of components in the film that is soluble in water. The incorporation of zein did not result in significant changes, where the TSM values ranged around from 45% to 50% for all zein concentrations. GG is the main component in the composite film that contributes to the soluble matter. While zein is hydrophobic and is not soluble in water, but soluble in alcohol [36]. So, all zein particles will remain in the undissolved composite film.

Water Vapour and Oxygen Barrier Properties

WVP and OP are important parameters in determining how well packaging can control water vapour and oxygen transmission. These two parameters have a direct impact on food product shelf life [37]. Therefore, the WVP and OP of composite films incorporated with various zein concentrations (0% - 20%) were analysed.

Pure GG film is highly permeable to water vapour and hence this control film has the highest WVP, 10.71×10^{-4} g mm m^{-2} h^{-1} kPa^{-1}. This is due to the hydrophilic nature of GG and GG will tend to attract water. It is observed that the addition of zein resulted in a significant ($p < 0.05$) reduction in WVP, where WVP reduced progressively from 9.29×10^{-4} $gmmm^{-2}h^{-1}kPa^{-1}$ to 7.96×10^{-4} $gmmm^{-2}h^{-1}kPa^{-1}$ for 5% to 20% zein, respectively. This is because zein is a hydrophobic protein and can act as moisture transfer barrier. These results are in good accordance with the WCA in this study. Where increasing zein concentration results in enhanced surface hydrophobicity. Increasing corn-zein concentration on polypropylene films decreases the WVP significantly and increased surface hydrophobicity [38]. These effects are attributed to the hydrophobic nature of zein. Moreover, incorporation of corn zein into salmon skin gelatin significantly decreased the WVP of composite film [39]. The authors suggest that zein hindered the hydrophilic sites in the composite film, which resulted in higher water-resistance.

Furthermore, the water-repelling effect of zein is not the only factor that affects WVP. The microstructure of composite film also plays an important role [40]. Results from FTIR show that when the concentration of zein increases, more intermolecular bonding, specifically hydrogen bond and electrostatic interactions were formed between zein and GG. This results in a denser network and suggest that the mobility of polymer chains decreases and the free volume in zein GG composite film reduced [41, 42]. Thus, migration of water molecules were impeded and WVP decreases when zein concentration increased.

Table 4. WVP, OP, swelling ratio, TSM, puncture force and deformation of zein-loaded GG film incorporated with various zein concentrations (0% - 20%).

Concentration of zein (%)	WVP ± SD × 10^{-4} (g mm m^{-2} h^{-1} kPa^{-1})	OP ± SD (m mol kg^{-1})	Swelling Ratio ± SD (%)	TSM ± SD (%)	Puncture Force ± SD (N)	Deformation ± SD (%)
0 (Control)	10.71 ± 0.12^{a}	30.89 ± 5.62^{a}	12791 ± 1463^{c}	50.23 ± 2.46^{a}	8.3168 ± 0.1612^{a}	2.84 ± 0.05^{ab}
5	9.29 ± 0.65^{b}	25.09 ± 0.51^{ab}	15641 ± 1854^{bc}	48.71 ± 6.57^{a}	8.4589 ± 0.4446^{a}	2.82 ± 0.06^{ab}
10	8.92 ± 0.57^{bc}	23.38 ± 0.78^{b}	16397 ± 2499^{ab}	44.21 ± 5.62^{a}	7.7678 ± 0.1488^{b}	2.95 ± 0.05^{a}
15	8.43 ± 0.19^{bc}	25.09 ± 0.51^{ab}	18284 ± 1724^{a}	47.52 ± 6.59^{a}	8.4159 ± 0.2099^{a}	2.87 ± 0.11^{a}
20	7.96 ± 0.38^{c}	22.38 ± 2.42^{b}	13684 ± 1105^{bc}	45.71 ± 6.22^{a}	7.6362 ± 0.0532^{b}	2.70 ± 0.10^{b}

^{abc} represents statistically significant differences of WVP, OP, swelling ratio, TSM, puncture force and deformation for zein-loaded GG film at various concentrations (0% - 20%) at $p < 0.05$; Values stated were mean ± SD with three replicates for WVP and OP, while five replicates for swelling ratio, TSM, puncture force and deformation.

The incorporation of zein significantly ($p < 0.05$) decreases the OP of GG film. As the OP of GG film is 30.89 ± 5.62 m mol kg^{-1} and after addition of 10% zein, the OP decreased significantly ($p < 0.05$) to 23.38 ± 0.78 m mol kg^{-1}. Moreover, the OP further reduced to 22.38 ± 2.42 m mol kg^{-1} when 20% zein was added. These results suggest that the presence of polar interaction in zein-loaded GG film microstructure and perpendicular layer is possibly produced [43]. In which, a tortuous path for oxygen molecules is created and this impedes the movement across composite film. The intercalated structure of zein contributes to the improvement of OP, which is in accordance with the results obtained in this study [44]. Besides, addition of zein will decrease the oxygen solubility and prevent delivery of oxygen. A study involves blending zein with chitosan film and a low OP is obtained. This is due to the decrease in oxygen solubility and travel of oxygen across film is obstructed [45].

Mechanical Properties

Puncture test and deformation are commonly performed to determine the maximum force required to penetrate food packaging materials. This is particularly important because when packaging is damaged, food products will be contaminated by external environment. In this study, pure GG film has a high puncture force of 8.3168 N. However, the addition of 10% and 20% zein reduced the puncture force significantly ($p < 0.05$) to 7.7678 N and 7.6362 N, respectively (Table 4). On the other hand, no significant changes were observed for addition of 5% and 15% zein. Most of the deformation of composite films are not affected by changes in zein concentration, except for 20% zein. Whereby the lowest deformation is obtained and significantly lower than 10% and 15% zein. Therefore, this implies that at higher zein concentration, which is after 10% zein addition, deformation decreases.

Microstructure of Zein-loaded GG Film

FESEM Analysis

The FESEM images of GG film in Figure 4a show that GG form films that have a coarse and irregular surface. Aggregated granules were formed with the size of a few micrometers [46]. For FESEM images of zein with GG film, zein appears to be a small, spherical structure and is well distributed across the GG film. This is likely attributed to zein, which is well dispersed in the GG mixture during mixing, which results in minimal aggregation [47].

When the concentration of zein increases, the small, spherical structure of zein on GG film also increases and hence they are more closely positioned to each other. The aggregated granules of GG also appears to be reduced as the concentration of zein increases. This suggests that incorporation of zein will affect the microstructure of GG film. Several studies also reported that when protein is incorporated into GG, intermolecular bonds, specifically hydrogen bonds and electrostatic interaction, are established [48, 49].

AFM analysis

Through AFM, the 3D surface topographic images of zein-loaded GG film were obtained. Figure 4a (i) and 4b (i) shows that pure GG film has an irregular surface and GG aggregated into large granules. This micro-structure is similar to the SEM image of pure GG film as mentioned in this study. Following the addition of 5% and 10% zein, the composite film surface have small bumps. These appear to be spherical zein particles. Meanwhile, the GG granules have become flattened and the 'peak and through' pattern started to diminish. At higher zein concentration, the zein particles become bigger as zein particles tend to aggregate. Although aggregation of zein had occurred, the zein particles are still well distributed across the GG film surface (Figure 4a (iv) and (v)).

The surface roughness of zein decreases at a lower concentration as for the R_a and R_q for pure GG film is 37.1 nm and 48.9 nm respectively. After adding 10% zein, the R_a and R_q of composite film decreased to 23.7 nm and 29.8 nm respectively. However, the roughness increases when zein concentrations increased to 20% with the R_a and R_q are 38.5 nm and 48.7 nm respectively. This increase in roughness at higher zein concentrations may be due to the increase in zein particle aggregation, which resulted in larger zein particle and protrude out to the surface [50]. A study that involves incorporation of zein in gelatin film also reported that the roughness increased gradually at higher zein percentage [14].

FTIR Analysis

FTIR elucidated the interactions of functional groups between GG and zein and the newly formed inter-molecular bonds. For pure GG film, the peaks at 3288 cm^{-1} represent the characteristic O-H stretch from the hydroxyl group. Pure GG film has the characteristic O-H stretch peak from hydroxyl group at around 3440 cm^{-1} [51, 52]. The shifting of O-H stretch peak in this study may be due to addition of glycerol. Whereby glycerol is a plasticizer that is rich in O-H hydroxyl group. This is similar in a study where addition of glycerol in gum cordia film, shifted the O-H hydroxyl group stretch from 3326 cm^{-1} to 3271 cm^{-1} [53]. Besides that, the peak at 1617 cm^{-1} represents absorptions of C=O stretch from carboxylate. The peaks at 2933 cm^{-1} and 2884 cm^{-1} represent the absorptions of C-H stretch. While peaks at 1410 cm^{-1} and 1726 cm^{-1} were attributed to C-H stretching of the methyl group and C=O stretching of alkyl ester, respectively [54].

The presence of zein results in a change of peak at 3288 cm^{-1}, 1617 cm^{-1} and 1534 cm^{-1}. For instance, the peak at 3288 cm^{-1}, which represents O-H stretch

from hydroxyl group that formed hydrogen bond, had minor shift to 3285 cm^{-1}. This peak small decreased to lower wavenumber indicates an increase in the hydrogen bonds formed between GG and zein [55]. Besides that, the peak at 1617 cm^{-1} in pure GG film had become broader and slightly shift to 1620 cm^{-1} and a new peak was formed at 1539 cm^{-1}. Both of these changes suggest that electrostatic interactions had occurred between GG and zein, as zein has an absorption peak at around 1655 cm^{-1} – 1645 cm^{-1} and 1547 cm^{-1} – 1558 cm^{-1}, which represents amide I and amide II respectively [56, 45]. Similar results were reported in applying zein/GG composite particles to stabilize emulsion and electrostatic interaction between zein and GG are formed [57]. Therefore, the intermolecular interaction between zein and GG not only involved hydrogen bonding, but electrostatic interactions also plays an important role.

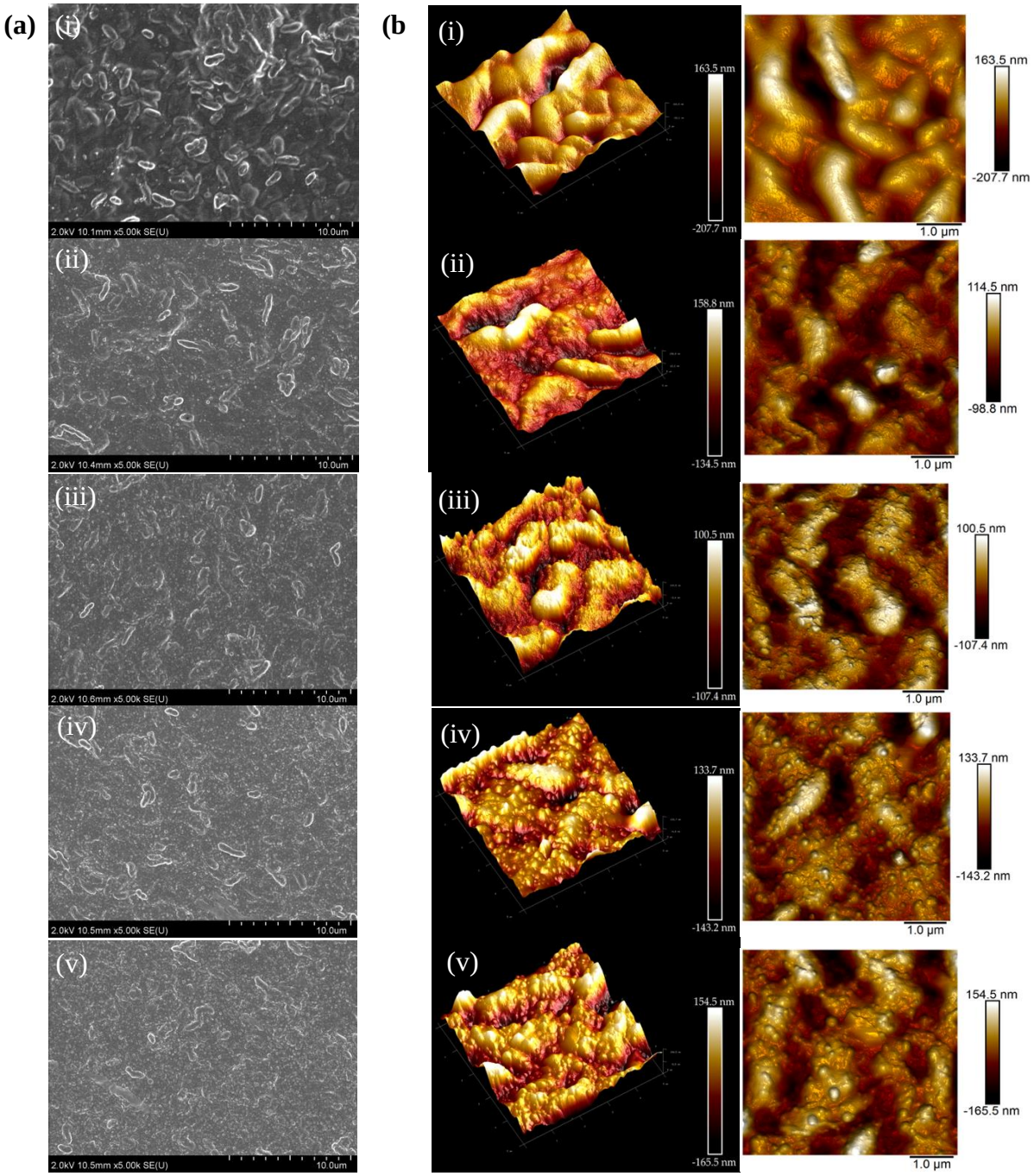

Figure 4. (a) FESEM images at × 5.00k magnification and **(b)** AFM surface topographic images at 5 × 5 µm scan size of GG film incorporated with various zein concentration (0% - 20%), with **(i)** 0% zein (Pure GG film); **(ii)** 5% zein + GG film; **(iii)** 10% zein + GG film; **(iv)** 15% zein + GG film; **(v)** 20% zein +GG film.

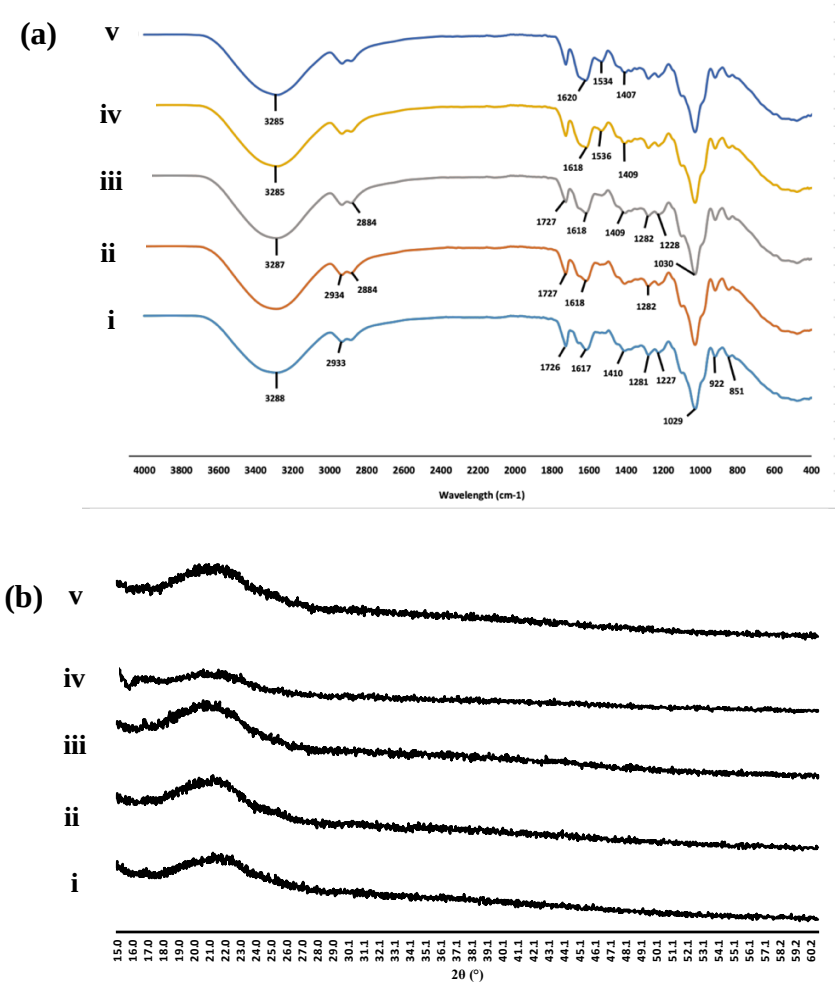

Figure 5. (a) FTIR spectrum at wavelength between 400 and 4000 cm^{-1} and **(b)** XRD pattern of GG film incorporated with various zein concentration (0% - 20%), with **(i)** 0% zein (pure GG film); **(ii)** 5% zein + GG film; **(iii)** 10% zein + GG film; **(iv)** 15% zein + GG film; **(v)** 20% zein + GG film**.**

XRD Analysis

The XRD pattern of all GG film incorporated with various zein concentrations (0% - 20%) exhibited a similar broad diffraction peak at 22.0° (Figure 5(b)). This characteristic diffraction peak of GG and the broad peak indicates that all composite films are having amorphous or semi – crystalline structure [58]. The crystallinity proportion in composite films are analysed by DIFFRAC.EVA (v4.2.1) software and the crystallinity value increased when the concentration of zein increased. The crystallinity value of 0% zein, 5% zein, 10% zein, 15% zein and 20% zein were 57.5%, 55.1%, 58.0%, 51.0% and 60.0% respectively. The increase in crystallinity value may be due to the presence of new intermolecular bonds formed between GG and zein, specifically hydrogen bonds and electrostatic interactions and this resulted in a more ordered structure formed. This is in accordance with our findings from FTIR analysis, where hydrogen bonds and electrostatic interactions increase when more zein is incorporated.

CONCLUSION

Zein-loaded GG film had been produced successfully through the solvent casting method and incorporation of zein improved the water-resistance performance and barrier properties of the composite film. Zein/GG FFS exhibited shear thinning behaviour and increasing zein concentration increases viscosity. Besides, zein/GG FFS also shows 'true-gel' behaviour, whereby G′ has a minimal dependency on angular frequency. The complex viscosity of zein/GG FFS increases with increasing zein concentration and this further confirms the results from the steady shear analysis. The surface hydrophobicity of GG film was improved when zein is added into GG film, with the water CA increased by almost 20%. In addition, the WVP also decreased with an increased zein concentration. The gas barrier properties were also enhanced, as presence of zein reduced the OP up to 28%. These findings were attributed to the hydrophobic nature of zein and the intermolecular interaction formed between zein and GG, which impedes the movement of water vapour

and oxygen molecules. Good compatibility between zein and GG were also determined by the results from FTIR, XRD, FESEM and AFM, where the intermolecular interactions, hydrogen bonds and electrostatic interactions were formed. Overall, this study had elucidated the great potential of this novel zein-loaded GG film as a biodegradable food packaging film, owing to its good water-resistance performance and barrier properties. Further study is required to improve these composite films' mechanical properties (puncture force and deformation).

ACKNOWLEDGEMENTS

This research was supported by the School of Science ECR Grant Scheme (ECR-000008), Monash University Malaysia. Teoh Ru Wei: Conceptualization, Methodology, Investigation, Writing – original draft, Visualization. Thoo Yin Yin: Conceptualization, Supervision, Writing – review and editing. Ting Su Yien, Adeline: Conceptualization, Supervision, Writing – review and editing.

REFERENCES

1. Mohamed, S. A. A., El-zSakhawy, M. & El-Sakhawy, M. A. M. (2020) Polysaccharides, Protein and Lipid -Based Natural Edible Films in Food Packaging: A Review. *Carbohydrate Polymers*, **238**, 116178. https://doi.org/10.1016/j.carbpol.2020.116178.

2. Muthukumar, T., Song, J. E. & Khang, G. (2019) Biological Role of Gellan Gum in Improving Scaffold Drug Delivery, Cell Adhesion Properties for Tissue. *Molecules*, **24(24)**, 4514. https://doi.org/10.3390/molecules24244514.

3. Saha, D. & Bhattacharya, S. (2010) Hydrocolloids as thickening and gelling agents in food: A critical review. *Journal of Food Science and Technology*, **47(6)**, 587–597. https://doi.org/10.1007/s13197-010-0162-6.

4. Kuo, M. S., Mort, A. J. & Dell, A. (1986) Identification and location of l-glycerate, an unusual acyl substituent in gellan gum. *Carbohydrate Research*, **156**, 173–187. https://doi.org/10.1016/S0008-6215(00)90109-5

5. Hayashi, M., Takei, R., Umene, S., Narita, K., Kato, K., Kobayashi, Y. & Honma, Y. (2016) Tribological analysis of the surface of food gels. *Food Hydrocolloids*, **58**, 343–346. https://doi.org/10.1016/j.foodhyd.2016.03.010

6. Akkineni, A., Ahlfeld, T., Funk, A., Waske, A., Lode, A. & Gelinsky, M. (2016) Highly Concentrated Alginate-Gellan Gum Composites for 3D Plotting of Complex Tissue Engineering Scaffolds. *Polymers*, **8(5)**, 170. https://doi.org/10.3390/polym8050170

7. Oliveira, I. M., Gonçalves, C., Shin, M. E., Lee, S., Reis, R. L., Khang, G. & Oliveira, J. M. (2021) Enzymatically crosslinked tyramine-gellan gum hydrogels as drug delivery system for rheumatoid arthritis treatment. *Drug Delivery and Translational Research*, **11(3)**, 1288–1300. https://doi.org/10.1007/s13346-020-00855-9.

8. Kuo, S. M., Chang, S. J., Wang, H. Y., Tang, S. C. & Yang, S. W. (2014) Evaluation of the ability of xanthan gum/gellan gum/hyaluronan hydrogel membranes to prevent the adhesion of postrepaired tendons. *Carbohydrate Polymers*, **114**, 230–237. https://doi.org/10.1016/j.carbpol.2014.07.049

9. Lee, H., Rukmanikrishnan, B. & Lee, J. (2019) Rheological, morphological, mechanical, and water-barrier properties of agar/gellan gum/montmorillonite clay composite films. *International Journal of Biological Macromolecules*, **141**, 538–544. https://doi.org/10.1016/j.ijbio mac.2019.09.021.

10. Zhang, N., Xu, J., Gao, X., Fu, X. & Zheng, D. (2017) Factors affecting water resistance of alginate/gellan blend films on paper cups for hot drinks. *Carbohydrate Polymers*, **156**, 435–442. https://doi.org/10.1016/j.carbpol.2016.08.101.

11. Balasubramanian, R., Kim, S. S. & Lee, J. (2018) Novel synergistic transparent k-Carrageenan/Xanthan gum/Gellan gum hydrogel film: Mechanical, thermal and water barrier properties. *International Journal of Biological Macromolecules*, **118**, 561–568. https://doi.org/10.1016/j.ijbiomac.2018.06.110.

12. Corradini, E., Curti, P. S., Meniqueti, A. B., Martins, A. F., Rubira, A. F., & Muniz, E. C. (2014). Recent advances in food-packing, pharmaceutical and biomedical applications of zein and zein-based materials. *International Journal of Molecular Sciences*, **15(12)**, 22438–22470. https://doi.org/10.3390/ijms151222438.

13. Parris, N. & Dickey, L. C. (2001) Extraction and solubility characteristics of zein proteins from dry-milled corn. *Journal of Agricultural and Food Chemistry*, **49(8)**, 3757–3760. https://doi.org/10.1021/jf0011790.

14. Ahammed, S., Liu, F., Khin, M. N., Yokoyama, W. H. & Zhong, F. (2020) Improvement of the water

resistance and ductility of gelatin film by zein. *Food Hydrocolloids*, **105**, 105804. https://doi.org/10.1016/j.foodhyd.2020.105804.

15. Wan, Z., Wang, L., Yang, X., Guo, J. & Yin, S. (2016) Enhanced water resistance properties of bacterial cellulose multilayer films by incorporating interlayers of electrospun zein fibers. *Food Hydrocolloids*, **61**, 269–276. https://doi.org/10.1016/j.foodhyd.2016.05.024.

16. Yin, Y. C., Yin, S. W., Yang, X. Q., Tang, C. H., Wen, S. H., Chen, Z., Xiao, B. jie & Wu, L. Y. (2014) Surface modification of sodium caseinate films by zein coatings. *Food Hydrocolloids*, **36**, 1–8. https://doi.org/10.1016/j.foodhyd.2013.08.027.

17. Brodnjak, U. V. & Tihole, K. (2020) Chitosan solution containing zein and essential oil as bio based coating on packaging paper. *Coatings*, **10(5)**. https://doi.org/10.3390/COATINGS10050497.

18. Teklehaimanot, W. H., Ray, S. S. & Emmambux, M. N. (2020) Characterization of pre-gelatinized maize starch-zein blend films produced at alkaline pH. *Journal of Cereal Science*, **95**, 103083. https://doi.org/10.1016/j.jcs.2020.103083.

19. Yousefi, A. R. & Ako, K. (2020) Controlling the rheological properties of wheat starch gels using epidium perfoliatum seed gum in steady and dynamic shear. *International Journal of Biological Macromolecules*, **143**, 928–936. https://doi.org/10.1016/j.ijbiomac.2019.09.153.

20. Ali Razavi, S. M., Alghooneh, A., Behrouzian, F. & Cui, S. W. (2016) Investigation of the interaction between sage seed gum and guar gum: Steady and dynamic shear rheology. *Food Hydrocolloids*, **60**, 67–76. https://doi.org/10.1016/j.foodhyd.2016.03.022.

21. Abdullah, Z. W. & Dong, Y. (2019) Biodegradable and water resistant poly(vinyl) alcohol (PVA)/ starch (ST)/glycerol (GL)/halloysite nanotube (HNT) nanocomposite films for sustainable food packaging. *Frontiers in Materials*, **6(58)**. https://doi.org/10.3389/fmats.2019.00058.

22. Ramezani, R. (2004) The effect of packaging materials and storage condition on the oxidative stability of refined sunflower oil. *Food Science and Technology Research*, **10(3)**, 350–354. https://doi.org/10.3136/fstr.10.350.

23. Nascimento, T. A., Calado, V. & Carvalho, C. W. P. (2012) Development and characterization of flexible film based on starch and passion fruit mesocarp flour with nanoparticles. *Food Research International*, **49(1)**, 588–595. https://doi.org/10.1016/j.foodres.2012.07.051.

24. Ghanbarzodeh, B., Oromiehie, A. R., Musavi, M., Falcone, P. M., D-Jomeh, Z. E. & Rad, E. R. (2007) Study of mechanical properties, oxygen permeability and AFM topography of zein films plasticized by polyols. *Packaging Technology and Science*, **20(3)**, 155–163. https://doi.org/10.1002/pts.750.

25. Pereda, M., Ponce, A. G., Marcovich, N. E., Ruseckaite, R. A. & Martucci, J. F. (2011) Chitosan-gelatin composites and bi-layer films with potential antimicrobial activity. *Food Hydrocolloids*, **25(5)**, 1372–1381. https://doi.org/10.1016/j.foodhyd.2011.01.001.

26. Qiao, D., Lu, J., Chen, Z., Liu, X., Li, M. & Zhang, B. (2023) Zein inclusion changes the rheological, hydrophobic and mechanical properties of agar/ konjac glucomannan based system. *Food Hydrocolloids*, **137**, 108365. https://doi.org/10.1016/j.foodhyd.2022.108365.

27. Zhang, L., Liu, Z., Han, X., Sun, Y., & Wang, X. (2019). Effect of ethanol content on rheology of film-forming solutions and properties of zein/ chitosan film. *International Journal of Biological Macromolecules*, ***134***, 807–814. https://doi.org/10.1016/j.ijbiomac.2019.05.085

28. Tian, L., Fan, H., Liu, H., Tong, Z., Liu, T. & Zhang, Y. (2021) Development and properties of zein/Tremella fuciformis polysaccharides blend as a hard capsule material. *Journal of Applied Polymer Science*, **138(46)**, 1–13. https://doi.org/10.1002/app.51379

29. Ali Razavi, S. M., Alghooneh, A., Behrouzian, F. & Cui, S. W. (2016) Investigation of the interaction between sage seed gum and guar gum: Steady and dynamic shear rheology. *Food Hydrocolloids*, **60**, 67–76. https://doi.org/10.1016/j.foodhyd.2016.03.022

30. Li, C., Xiang, F., Wu, K., Jiang, F. & Ni, X. (2020) Changes in microstructure and rheological properties of konjac glucomannan/zein blend film-forming solution during drying. *Carbohydrate Polymers*, **250**, 116840. https://doi.org/10.1016/j.carbpol.2020.116840

31. Altan, A. & Çayır, Ö. (2020) Encapsulation of carvacrol into ultrafine fibrous zein films via electrospinning for active packaging. *Food*

Packaging and Shelf Life, **26**. https://doi.org/10.1016/j.fpsl.2020.100581.

32. Law, K. Y. (2014) Definitions for Hydrophilicity, Hydrophobicity, and Superhydrophobicity: Getting the Basics Right. *Journal of Physical Chemistry*, **5(4)**, 686–688. https://doi.org/10.1021/jz402762h.

33. Huang, D., Zheng, Y., Zhang, Z., Quan, Q. & Qiang, X. (2020) Synergistic effect of hydrophilic palygorskite and hydrophobic zein particles on the properties of chitosan films. *Materials and Design*, **185**, 108229. https://doi.org/10.1016/j.matdes.2019.108229.

34. Shalom, T. ben, Belsey, S., Chasnitsky, M. & Shoseyov, O. (2021) Cellulose nanocrystals and corn zein oxygen and water vapor barrier biocomposite films. *Nanomaterials*, **11(1)**, 1–16. https://doi.org/10.3390/nano11010247.

35. Farajpour, R., Emam Djomeh, Z., Moeini, S., Tavahkolipour, H. & Safayan, S. (2020) Structural and physico-mechanical properties of potato starch-olive oil edible films reinforced with zein nanoparticles. *International Journal of Biological Macromolecules*, **149**, 941–950. https://doi.org/10.1016/j.ijbiomac.2020.01.175.

36. Li, Y., Li, J., Xia, Q., Zhang, B., Wang, Q. & Huang, Q. (2012) Understanding the dissolution of α-zein in aqueous ethanol and acetic acid solutions. *Journal of Physical Chemistry B*, **116(39)**, 12057–12064. https://doi.org/10.1021/jp305709y.

37. Cazón, P., Vázquez, M. & Velazquez, G. (2018) Novel composite films based on cellulose reinforced with chitosan and polyvinyl alcohol: Effect on mechanical properties and water vapour permeability. *Polymer Testing*, **69**, 536–544. https://doi.org/10.1016/j.polymertesting.2018.06.016.

38. Tihminlioglu, F., Atik, I. D. & Özen, B. (2010) Water vapor and oxygen-barrier performance of corn-zein coated polypropylene films. *Journal of Food Engineering*, **96(3)**, 342–347. https://doi.org/10.1016/j.jfoodeng.2009.08.018

39. Fan, H. Y., Duquette, D., Dumont, M. J. & Simpson, B. K. (2018) Salmon skin gelatin-corn zein composite films produced via crosslinking with glutaraldehyde: Optimization using response surface methodology and characterization. *International Journal of Biological Macromolecules*, **120**, 263–273. https://doi.org/10.1016/j.ijbiomac.2018.08.084.

40. Masamba, K., Li, Y., Hategekimana, J., Liu, F., Ma, J. G. & Zhong, F. (2016) Effect of type of plasticizers on mechanical and water barrier properties of transglutaminase cross-linked zein–oleic acid composite films. *International Journal of Food Engineering*, **12(4)**, 365–376. https://doi.org/10.1515/ijfe-2015-0289.

41. Chambi, H. & Grosso, C. (2006) Edible films produced with gelatin and casein cross-linked with transglutaminase. *Food Research International*, **39(4)**, 458–466. https://doi.org/10.1016/j.foodres.2005.09.009.

42. Garavand, F., Rouhi, M., Razavi, S. H., Cacciotti, I. & Mohammadi, R. (2017) Improving the integrity of natural biopolymer films used in food packaging by crosslinking approach: A review. *International Journal of Biological Macromolecules*, **104**, 687–707. https://doi.org/10.1016/j.ijbiomac.2017.06.093.

43. Valencia-Sullca, C., Vargas, M., Atarés, L. & Chiralt, A. (2018) Thermoplastic cassava starch-chitosan bilayer films containing essential oils. *Food Hydrocolloids*, **75**, 107–115. https://doi.org/10.1016/j.foodhyd.2017.09.008.

44. Ozcalik, O. & Tihminlioglu, F. (2013) Barrier properties of corn zein nanocomposite coated polypropylene films for food packaging applications. *Journal of Food Engineering*, **114(4)**, 505–513. https://doi.org/10.1016/j.jfoodeng.2012.09.005.

45. Zhang, L., Liu, Z., Wang, X., Dong, S., Sun, Y. & Zhao, Z. (2019) The properties of chitosan/zein blend film and effect of film on quality of mushroom (Agaricus bisporus). *Postharvest Biology and Technology*, **155**, 47–56. https://doi.org/10.1016/j.postharvbio.2019.05.013.

46. Wei, Y. C., Cheng, C. H., Ho, Y. C., Tsai, M. L. & Mi, F. L. (2017) Active gellan gum/purple sweet potato composite films capable of monitoring pH variations. *Food Hydrocolloids*, **69**, 491–502. https://doi.org/10.1016/j.foodhyd.2017.03.010.

47. Oymaci, P. & Altinkaya, S. A. (2016) Improvement of barrier and mechanical properties of whey protein isolate based food packaging films by incorporation of zein nanoparticles as a novel bionanocomposite. *Food Hydrocolloids*, **54**, 1–9. https://doi.org/10.1016/j.foodhyd.2015.08.030.

48. Picone, C. S. F. & da Cunha, R. L. (2010)

Interactions between milk proteins and gellan gum in acidified gels. *Food Hydrocolloids*, **24(5)**, 502–511. https://doi.org/10.1016/j.foodhyd.2009.12.007.

49. Pires Vilela, J. A., Cavallieri, Â. L. F. & Lopes da Cunha, R. (2011) The influence of gelation rate on the physical properties/structure of salt-induced gels of soy protein isolate-gellan gum. *Food Hydrocolloids*, **25(7)**, 1710–1718. https://doi.org/10.1016/j.foodhyd.2011.03.012.

50. Chatsisvili, N., Philipse, A. P., Loppinet, B. & Tromp, R. H. (2017) Colloidal zein particles at water-water interfaces. *Food Hydrocolloids*, **65**, 17–23. https://doi.org/10.1016/j.foodhyd.2016.10.036.

51. Xu, X., Li, B., Kennedy, J. F., Xie, B. J. & Huang, M. (2007) Characterization of konjac glucomannan-gellan gum blend films and their suitability for release of nisin incorporated therein. *Carbohydrate Polymers*, **70(2)**, 192–197. https://doi.org/10.1016/j.carbpol.2007.03.017.

52. Du, Y., Sun, J., Wang, L., Wu, C., Gong, J., Lin, L., Mu, R. & Pang, J. (2019) Development of antimicrobial packaging materials by incorporation of gallic acid into Ca2+ crosslinking konjac glucomannan/gellan gum films. *International Journal of Biological Macromolecules*, **137**, 1076–1085. https://doi.org/10.1016/j.ijbiomac.2019.06.079.

53. Haq, M. A., Hasnain, A. & Azam, M. (2014) Characterization of edible gum cordia film: Effects of plasticizers. *LWT - Food Science and Technology*, **55(1)**, 163–169. https://doi.org/10.1016/j.lwt.2013.09.027.

54. Vijan, V., Kaity, S., Biswas, S., Isaac, J. & Ghosh, A. (2012) Microwave assisted synthesis and characterization of acrylamide grafted gellan, application in drug delivery. *Carbohydrate Polymers*, **90(1)**, 496–506. https://doi.org/10.1016/j.carbpol.2012.05.071.

55. Wang, K., Wu, K., Xiao, M., Kuang, Y., Corke, H., Ni, X. & Jiang, F. (2017) Structural characterization and properties of konjac glucomannan and zein blend films. *International Journal of Biological Macromolecules*, **105**, 1096–1104. https://doi.org/10.1016/j.ijbiomac.2017.07.127.

56. Chen, G., Ali, F., Dong, S., Yin, Z., Li, S. & Chen, Y. (2018) Preparation, characterization and functional evaluation of chitosan-based films with zein coatings produced by cold plasma. *Carbohydrate Polymers*, **202(29)**, 39–46. https://doi.org/10.1016/j.carbpol.2018.08.122.

57. Jiang, Y., Zhang, C., Yuan, J., Wu, Y., Li, F., I. N. Waterhouse, G., Li, D. & Huang, Q. (2021) Exploiting the robust network structure of zein/low-acyl gellan gum nanocomplexes to create Pickering emulsion gels with favorable properties. *Food Chemistry*, **349**, 129112. https://doi.org/10.1016/j.foodchem.2021.129112.

58. Yang, F., Xia, S., Tan, C. & Zhang, X. (2013) Preparation and evaluation of chitosan-calcium-gellan gum beads for controlled release of protein. *European Food Research and Technology*, **237(4)**, 467–479. https://doi.org/10.1007/s00217-013-2021-y.